Eur J Drug Metab Pharmacokinet (2016) 41:627–635
DOI 10.1007/s13318-015-0284-3

ORIGINAL PAPER

Chronopharmacokinetics of Erlotinib and Circadian Rhythms of Related Metabolic Enzymes in Lewis Tumor-Bearing Mice

Jiao Liu[2] · Chun-Yan Wang[1] · Song-Gang Ji[1] · Xia Xu[1] · Pei-Pei Wang[5] · Bin Zhang[6] · Li-Yan Zhao[1] · Liang Liu[3] · Ping-Ping Lin[3] · Le-Kun Liu[4] · Ming-Chun Li[1]

Published online: 19 July 2015

Abstract
Objective The purpose of the current study was to investigate the effect of the dosing time on the pharmacokinetics of erlotinib and the circadian rhythms of the metabolism enzymes in tumor-bearing mice.
Methods Female C57BL mice were randomly assigned to six groups. Erlotinib was orally administrated to the mice in each group at six different times of day. The plasma concentration of erlotinib was determined through a high-performance liquid-chromatographic assay, and the total mRNA was extracted from liver tissues to determine the expression of the mRNA of the related drug metabolism enzymes by qRT-PCR.
Results The results indicated that $AUC_{0-24\ h}$ and $MRT_{0-24\ h}$ were the lowest in the 20:00 group ($P < 0.01$). T_{max} of the 13 HALO (hour after light onset), 17 HALO and 21 HALO groups was higher than that of the 1 HALO and 5 HALO groups ($P < 0.01$). CL of the light-phase groups was lower than that of the dark-phase groups ($P < 0.01$). The peak value of C_{max} appeared in the 5 HALO group ($P < 0.01$). The mRNA levels of Cyp3a11, Cyp3a13 and Cyp1a2 were generally higher during the afternoon and the dark phase.
Conclusion Circadian rhythm plays a critical role in the pharmacokinetics of erlotinib in mice, and the mechanisms may be attributed to gene expression rhythms of drug-metabolizing enzymes in liver tissues.

1 Introduction

It has been well recognized that almost all living organisms, including plants, animals, bacteria and fungi, are functioning along certain cycles or circadian rhythms. Daily activities such as sleep, metabolism, hormonal secretion and cellular proliferation are controlled by these endogenous rhythms [1]. Chronopharmacology is a subject that explores the interaction of medication and the biologic rhythmic events. The traditional administration regimen divides the total daily dosage evenly into several times, based on the assumption that the physiological function, pathology of the body and drug effect remain constant during 24 h. However, with recent advances in chronopharmacology, new rigorous scientific regimens have been proposed, and the old even-division precepts are now being replaced by chronotherapy.

The efficacy and tolerability of a drug vary with administration time, which is related to the circadian rhythms of biochemical, physiological and behavioral processes. Indeed, many diseases such as asthma [2, 3], allergic rhinitis [4], cardiovascular diseases [5, 6] and cancer [7, 8] demonstrate circadian patterns in the occurrence or intensity of symptoms. Therefore, different dosing times of drugs for these diseases may demonstrate various effects. For example, aspirin [9, 10], torasemide [11], ramipril [12] and amlodipine/valsartan

✉ Ming-Chun Li
lmc401y@163.com

1 Department of Pharmacy, No. 401 Hospital of Chinese People's Liberation Army, Qingdao, Shandong, China

2 Department of Pharmacy, Affiliated Hospital of Weifang Medical University, Weifang, Shandong, China

3 Department of Pharmacology, Medical College of Qingdao University, Qingdao, Shandong, China

4 Weifang Institute of Dermatology, Weifang, Shandong, China

5 School of Pharmacy, Fudan University, Shanghai, China

6 Institute of Medicinal Plant Development, Peking Union Medical College and Chinese Academy of Medical Sciences, Beijing, China

combination [13] are more effective when administrated at bedtime; prednisone MR [14] and simvastatin [15] should be given in the evening, while the night time is believed to be superior to other times for nebicapone [16, 17].

Chrono-chemotherapy is based on the therapy of chronopharmacology, researching the rhythms of drugs and the body in order to improve the effect and reduce toxicity. Dihydropyrimidine dehydrogenase (DPD, a rate-limiting enzyme of 5-fluorouracil) has been found to display remarkable circadian rhythms, and the activity of the enzyme is higher during midnight to 10:00 in the morning [18]. The present universal administration regimen of 5-fluorouracil is continuous intravenous infusion from 22:00 to 10:00, and the T_{max} appears at 4:00, which predicts a better efficacy.

Erlotinib (TARCEVA) is a small molecule-targeting inhibitor, which suppresses the intracellular phosphorylation of tyrosine kinase associated with the epidermal growth factor receptor (EGFR). Erlotinib is metabolized mainly by CYP3A4 in the liver, and only a small part is metabolized by CYP1A2 and CYP1A1. An optimal study compared the efficacy and tolerability of erlotinib versus standard chemotherapy in the first-line treatment of patients with advanced EGFR mutation-positive NSCLC. The result indicated that erlotinib conferred a significant progression-free survival benefit and was associated with more favorable tolerability [19]. Erlotinib is the only TKI that has been proved to significantly prolong progression-free survival in NSCLC patients. However, none of the previous studies have determined circadian-dependent variations of erlotinib thus far. In the present study, we investigated the chronopharmacokinetic characters of erlotinib in Lewis tumor-bearing mice. Moreover, we also determined the expression of Cyp3a11, Cyp3a13 and Cyp1a2, which are homologs of CYP3A4 and CYP1A2 in the human body, in order to identify whether the enzymes display a circadian oscillation.

2 Materials and Methods

2.1 Materials

Erlotinib hydrochloride tablets (Tarceva, Schwarz Pharma Manufacturing Inc., Chinese Drug Approval No. J20090116, 150 mg). The tablets were suspended in 0.5 % CMC-Na solution to a final concentration of 15 mg/ml after the coating was removed. Erlotinib hydrochloride standard (purity = 98 %) and sorafenib standard (internal standard, purity = 98 %) were purchased from Toronto Research Chemicals Inc. (TRC, Toronto, Canada). Analytical grade *n*-hexane and ethyl acetate were purchased from Aibi Chemistry Preparation Co., Ltd. (Shanghai, China). HPLC-grade acetonitrile was from Shield Fine Chemical Products Co., Ltd. (Tianjin, China). All the other reagents were of analytical grade.

The StarSpin animal mRNA kit was purchased from Genstar Biosolutions Co., Ltd., China. The PrimeScript®-RT reagent kit with gDNA Eraser and SYBR® Premix Ex TaqTM were purchased from Takara Biotechnology (Dalian) Co., Ltd., China.

2.2 Animals and Cells

Female C57BL/6 mice, 4 weeks old, were obtained from Vital River Laboratory [Beijing, China; approval no. SCXK (Beijing) 2012-0001]. The mice were housed under standardized 12 h-light/dark cycle conditions (lights on at 7:00 a.m., off at 7:00 p.m., 500 lux and 25 lux, were controlled during the light span and dark span, respectively) at 24 ± 2 °C and 70 ± 10 % humidity with food and water available ad libitum [20–22]. All mice were synchronized for 3 weeks.

Lewis lung cancer (LLC) cells (ATCC, USA) were obtained from Beinachuanglian Biological Science Institute (Beijing, China) and were passaged in vitro to reach a proper quantity before the implantation. Three weeks later, the tumor cells were suspended, and a 0.2 ml volume of approximately 1×10^6 to 1×10^7 viable cells was inoculated subcutaneously into the right groin of the mice [22, 23].

2.3 Experimental Design

Ten days after the inoculation, a total of 504 tumor-bearing mice were randomly assigned into six circadian groups, with 84 animals in each group. All the mice of six groups were orally given 0.2 ml erlotinib hydrochloride suspension at 1 HALO (hours after light onset), 5 HALO, 9 HALO, 13 HALO, 17 HALO and 21 HALO, respectively. Seven tumor-bearing mice without the administration and another three normal mice were added to each circadian group as model and blank controls, respectively. The six circadian groups were further divided into 12 subgroups of 7 mice each to study the plasma erlotinib concentrations over time. Blood was taken at 5, 10, 20, 30, 45 min, 1.5, 3, 5, 8, 12, 16 and 24 h after each administration with one subgroup at a time. All the mice were killed immediately after their blood had been taken. Blood samples were collected in 2 ml heparinized tubes and centrifuged at 4000 r/min for 10 min at room temperature. The plasma was separated and stored at −86 °C before analysis. The liver tissue samples were taken from three mice of the subgroups that were killed at 30 min, 1.5, 3, 8, 12, 16 and 24 h after administration. The livers of corresponding controls were taken at 8:00, 12:00, 16:00, 20:00, 24:00 and 4:00, respectively, on the same experimental day. The tissue samples were immediately frozen in liquid nitrogen for 15 min and then stored at −86 °C.

2.4 Pharmacokinetics

2.4.1 Chromatographic Methods

Erlotinib and sorafenib were determined by an Agilent 1260 Infinity LC (Agilent, USA), and the stationary phase consisted of a ZORBAX SB-C18 column (5 μm, 4.6 × 250 mm, Agilent) and a guard column (5 μm, 4.6 × 12.5 mm, Agilent) of the same packing.

The elution was performed using the mobile phase consisting of a mixture of acetonitrile and water (55:45, v/v), with the pH adjusted to 2.0 (trifluoroacetic acid) [24]. The flow rate was 1.0 ml/min and the total running time was 15 min. The column temperature was maintained at 25 °C. Sample volumes of 20 μl were injected, and erlotinib was detected by the UV absorbance at 250 nm.

Stock solution, calibration standards and quality controls: Erlotinib and IS were dissolved in the mobile phase and diluted to a final concentration of 456 and 85.2 μg/ml, respectively. All stock solutions were stored at 4 °C. Standard solutions of erlotinib were prepared by diluting stock solutions into eight concentrations of 446,880, 223,440, 148,960, 111,720, 74,480, 27,930, 13,965 and 4655 ng/ml. The quality control (QC) samples of 558.60 ng/ml (LQC), 4468.80 ng/ml (MQC) and 35,750.40 ng/ml (HQC) were prepared in the same manner.

2.4.2 Sample Preparation

Mouse plasma (100-μl aliquot each) was transferred to a 1.5 ml polypropylene microcentrifuge tube. Then 20 μl of IS (85.2 μg/ml) and 50 μl of NaOH (0.1 N) were added to this aliquot. Next, 1 ml of hexane–ethyl acetate (30:70, v/v) was added, and the mixture was vortexed for 5 min followed by centrifugation at 12,000 r/min for 10 min at room temperature. The supernatant was transferred into a new 1.5-ml polypropylene microcentrifuge tube and evaporated to dryness at 40 °C under a nitrogen stream. The residue was reconstituted in 100 μl of mobile phase.

Pharmacokinetic analysis and statistical analysis: The concentration of erlotinib in the plasma was determined as described above, and the concentration-time curve of each administration time was drawn accordingly. WinNonlin was employed to calculate the pharmacokinetic parameters of all the groups. Finally, the pharmacokinetic parameters of the six circadian groups were compared by analyses of variance (ANOVA, F value). The differences between the means were considered statistically significant when $P < 0.05$.

2.5 Gene Expressions of *Cyp3a11*, *Cyp3a13* and *Cyp1a2*

2.5.1 Total RNA Preparation and Primer Design

Total RNA was extracted from the tissue samples by using StarSpin animal mRNA kits according to the manufacturer's protocol. The complementary DNA (cDNA) was synthesized using the PrimeScript® RT reagent kit according to the manufacturer's instructions. The primers of the three genes and *GAPDH*, which was used as internal control because of its stable expression level in liver cells, were designed by UCSC Genome Browser.

2.5.2 qRT-PCR

The PCR reaction mixture contained 12.5 μl SYBR®-Premix Ex TaqTM, 5 μM PCR forward primer and PCR reverse primer, 1 μl cDNA and 9.5 μl dH_2O, adding up to a final volume of 25 μl. The specificity of PCR amplification was analyzed by the melting curve.

Each sample was run in triplicate in a TL988 Real-Time Quantitative PCR (Xi'an Tianlong Science and Technology Co., Ltd.). The threshold cycle, ΔCt, was calculated as Ct (target gene) − Ct (*GAPDH*). The relative changes in the target genes in different treatment groups were determined by the formula $2^{-\Delta\Delta Ct}$, where ΔΔCt was calculated as follows:

$$\Delta\Delta Ct = \Delta Ct\ (\text{blank control}) - \Delta Ct\ (\text{circadian group})$$

ANOVA was conducted to compare the variation of mRNA expression of the three drug metabolic enzymes for 24 h after six administration time points.

3 Results

3.1 Determination of Erlotinib by Chromatography

Representative chromatograms of blank mouse plasma, the internal standard in the mobile phase and a sample of erlotinib in mouse plasma are shown in Fig. 1. Erlotinib ($t_R = 2.9$ min) and the internal standard sorafenib ($t_R = 11.6$ min) were well separated, and no significant interference from endogenous or exogenous compounds was observed in these chromatograms.

3.2 Linearity and Limit of Quantitation

Calibration curves were linear over the range of 465.5–44,688 ng/ml. The assay showed good correlation coefficients ($r^2 > 0.99$). Erlotinib's limit of quantitation was 465.5 ng/ml.

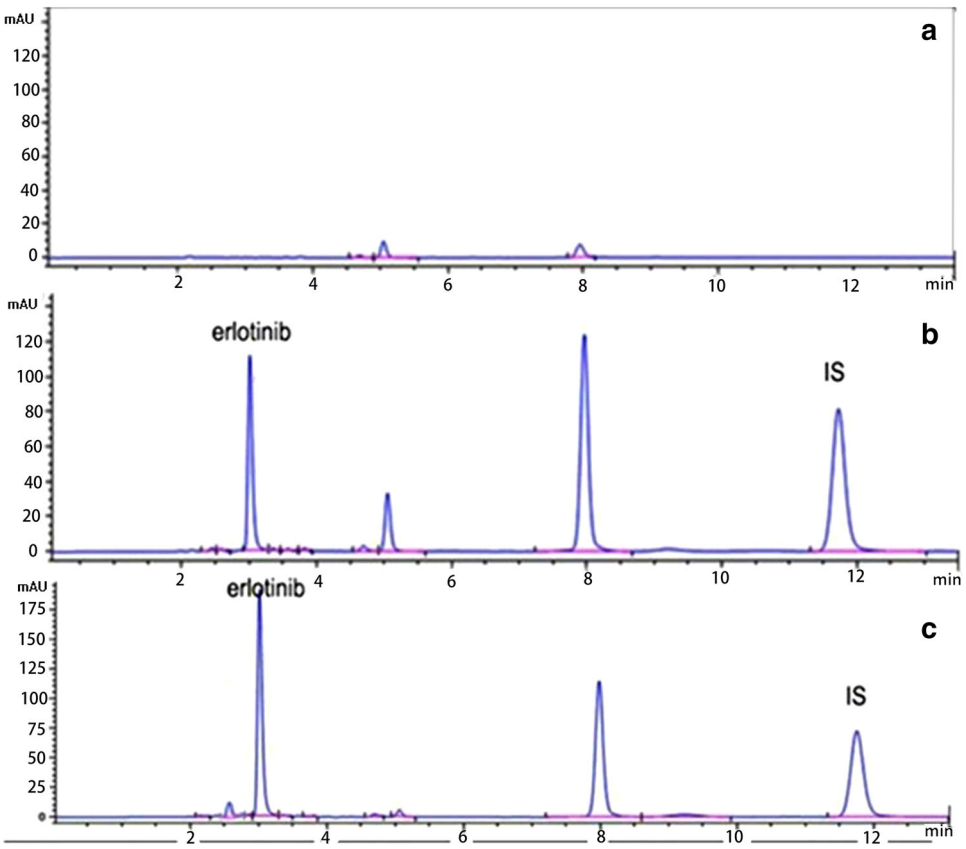

Fig. 1 Determination of erlotinib by chromatography. **a** Blank mouse plasma. **b** Blank plasma containing erlotinib and sorafenib (the concentration of erlotinib was 14,896 μg/l and that of sorafenib was 17,040 μg/l). **c** Plasma sample after administration (the concentration of erlotinib was 22,500 μg/l and that of sorafenib was 17,040 μg/l)

3.3 Accuracy, Precision and Recovery

Intra- and inter-assay bias and precision are shown in Table 1. For the high and medium level, the intra- and inter-assay precision was lower than 15 %, and the low level was under 20 %. The mean intra- and inter-assay accuracy was below 20 % at all levels. The samples are shown in Table 2.

3.4 Pharmacokinetic Parameters

The plasma concentration-time profile of erlotinib after administration at six different time of day is shown in Fig. 2. Table 3 summarizes the different pharmacokinetic parameters (mean grade ± SD) of erlotinib in mouse plasma after a single dose of 150 mg/kg at 1 HALO, 5 HALO, 9 HALO, 13 HALO, 17 HALO and 21 HALO. The study showed that the 13 HALO group was the lowest in both $AUC_{0-24\ h}$ and $MRT_{0-24\ h}$ compared to the other groups ($P < 0.01$), while the 1 HALO group and 5 HALO group were significantly higher than the others ($P < 0.01$). T_{max} of the 13 HALO, 17 HALO and 21 HALO groups was significantly lower than that of the 1 HALO, 5 HALO and 9 HALO groups ($P < 0.01$) and the 1 HALO group appeared the highest. C_{max} was the highest in the 5 HALO group and the lowest in the 13 HALO group ($P < 0.01$). As for CL, the 13 HALO group appeared to be the highest and the 9 HALO group the lowest ($P < 0.01$). Moreover, the $t_{1/2}$ of the 1 HALO group was significantly lower than those of all the other groups, while the 9 HALO group showed the highest, which was nearly three times that of the 1 HALO group ($P < 0.01$). The Vz/F of the 1 HALO group was the lowest compared with the other groups, and the 13 HALO group appeared the highest ($P < 0.01$).

Table 1 Precision, accuracy and recovery

Erlotinib (μg/l)	Within-day precision	RSD (%)	RE (%)	Between-day precision	RSD (%)	RE (%)	Recovery (%)
35,750.4	40,366 ± 2718	6.7	12.9	40,878 ± 1913	4.7	14.3	92.4 ± 7.2
4468.8	4861 ± 442	9.1	8.8	4674 ± 311	6.7	4.6	96.5 ± 4.7
558.6	480 ± 75	15.7	−14.1	467 ± 66	14.1	−16.4	88.0 ± 4.7

Mean grade ± SD, $n = 15$

Table 2 Sample stability

Erlotinib (μg/l)	Room temperature storage	RSD (%)	RE (%)	Repeated freezing and thawing	RSD (%)	RE (%)	Low temperature storage	RSD (%)	RE (%)
35,750.4	41,028 ± 791	1.92	14.8	40,824 ± 946	2.31	14.2	39,527 ± 465	1.18	10.6
4468.8	4330 ± 272	6.28	−3.11	4809 ± 395	8.21	7.61	4423 ± 245	5.54	1.02
558.6	475 ± 27	5.68	−15.0	515 ± 81	15.7	−7.81	483 ± 72	14.8	−13.5

Mean grade ± SD, $n = 15$

Room temperature storage: 22 °C

Repeated freezing and thawing: −20 to 37 °C

Low temperature storage: −86 °C

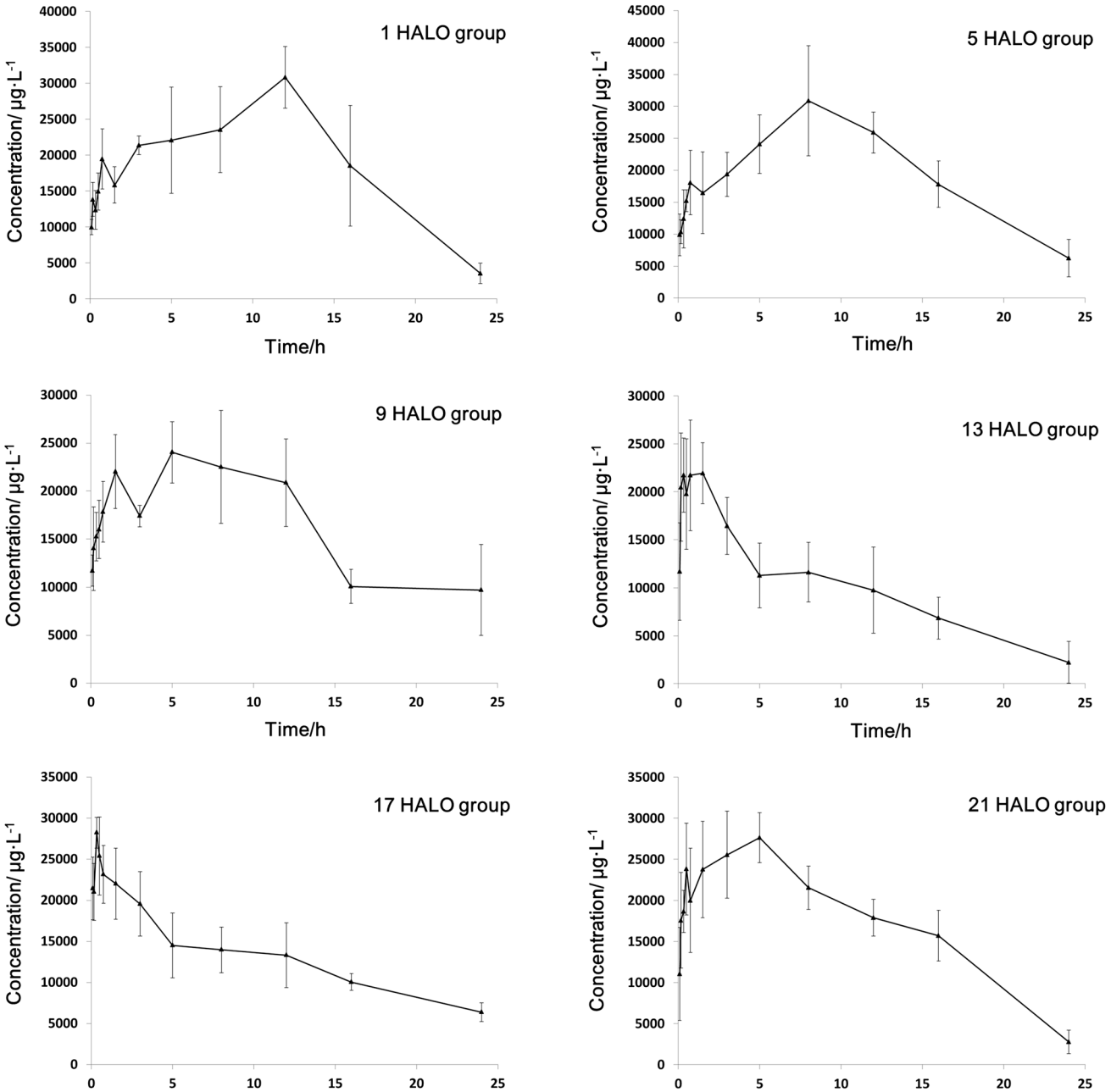

Fig. 2 Plasma concentration-time profile of erlotinib after administration at six different times of day

Table 3 Plasma pharmacokinetic parameters of erlotinib after administration at six circadian times in mice

Administration time	1 HALO	5 HALO	9 HALO	13 HALO	17 HALO	21 HALO
$AUC_{(0-24\ h)}$ (μg·h/l)	440,083 ± 26,150	450,289 ± 33,853	405,830 ± 36,763	229,242 ± 32,352$^{*,\#}$	304,308 ± 41,876$^{*,\#}$	431,361 ± 32,660
$AUC_{(0-\infty)}$ (μg·h/l)	462,181 ± 25,431	547,425 ± 60,772	628,669 ± 284,245	273,479 ± 55,001$^{*,\#}$	405,631 ± 63,253$^{*,\#}$	601,666 ± 199,793
$MRT_{(0-24\ h)}$ (h)	10.2 ± 0.6	10.3 ± 0.5	9.9 ± 0.8	8.2 ± 0.7$^{*,\#}$	8.4 ± 1.3$^{*,\#}$	9.6 ± 0.2
$MRT_{(0-\infty)}$ (h)	11.3 ± 0.5	14.9 ± 3.2	21.4 ± 11.7	13.1 ± 5.1	15.2 ± 4.8	19.0 ± 11.8
T_{max} (h)	12.8 ± 1.8	7.4 ± 1.3	5.8 ± 5.1	1.8 ± 0.3$^{*,\#,\Delta}$	0.6 ± 0.5$^{*,\#,\Delta}$	5.6 ± 1.2$^{*,\#,\Delta}$
CLz/*F* (l/h/kg)	0.325 ± 0.018$^{**,\Delta\Delta}$	0.277 ± 0.032$^{**,\Delta\Delta}$	0.267 ± 0.078$^{**,\Delta\Delta}$	0.568 ± 0.123	0.377 ± 0.062**	0.269 ± 0.078$^{**,\Delta\Delta}$
C_{max} (μg/l)	32,087 ± 2757*	32,893 ± 4579$^{\#}$	24,022 ± 2147$^{*,\#}$	22,561 ± 1226$^{*,\#}$	28,675 ± 1898$^{*,\#}$	27,631 ± 1749$^{*,\#}$
$t_{1/2}$ (h)	4.9 ± 1.7$^{\#\#}$	8.3 ± 2.5	13.9 ± 7.9$^{\#\#}$	8.7 ± 5.3	9.9 ± 4.2	11.7 ± 8.8
Vz/*F* (l/kg)	2.3 ± 0.733$^{\#\#}$	3.3 ± 0.724$^{\Delta,**,\Delta\Delta}$	4.7 ± 1.3$^{\#\#}$	6.6 ± 3.3$^{\#\#}$	5.2 ± 1.6$^{\#\#}$	3.8 ± 1.7$^{\#,**,\Delta\Delta}$

Each value represents the mean grade ± SD of seven mice

* $P < 0.01$, compared with the 5 HALO administration groups

\# $P < 0.01$, compared with the 1 HALO administration group

Δ $P < 0.01$, compared with the 9 HALO administration groups

** $P < 0.01$, compared with the 13 HALO administration groups

$\Delta\Delta$ $P < 0.01$, compared with the 17 HALO administration groups

\#\# $P < 0.01$, compared with all the other groups

3.5 Expression Levels of the Three Metabolic Enzymes

The overall expression level of *Cyp1a2* of the 20:00 group was the highest. Although the mRNA expressions of the other five groups were also slightly increased at 16 and 24 h, the variations were not significant.

The overall mRNA expression level of *Cyp3a13* of the 12:00 administration group was higher than those of all the other groups.

As for the *Cyp3a11*, the overall gene expression levels of the 12:00 group and 16:00 group were higher than for the other groups.

Figure 4 shows that the expression of *Cyp3a13* and *Cyp1a2* shows significant rhythms under normal circumstances. For *Cyp3a13*, the peak expression level appeared at 12:00 and 16:00, and for *Cyp1a2*, 20:00 was the climax time. However, there seemedto be no significant variation of *Cyp3a11* expression during 24 h.

4 Discussion and Conclusion

The high AUC, MRT and C_{max} of the 8:00 and 12:00 groups indicated that the bioavailability of erlotinib was higher when administrated at this period, and the action time was longer. However, the T_{max} of these two groups was also higher than in the other groups, especially the 20:00 and 24:00 groups, which means that the absorption speed was significantly lower during the morning. On the contrary, the low AUC, MRT and C_{max} and high CL of the 20:00 and 24:00 groups led to relatively bad bioavailability.

When comparing Figs. 3 and 4, it can be found that the original mRNA expression of *Cyp3a13* reached a high level at 12:00 and 16:00 (without drugs), while the overall expression during 24 h of *Cyp3a13* of the 12:00 (5 HALO) administration group and the 16:00 (9 HALO) administration group was also higher than in the other administration groups. Therefore, we concluded that the mRNA expression of *Cyp3a13* will increase if the drug is administrated at 12:00 and 16:00.

Higher Cyp enzyme activities during the dark phase have been previously observed in mouse livers [25]. Zhang et al. [26] demonstrated that the mRNA levels of several major Cyp enzymes were more highly expressed at night, which is in line with our current study.

Erlotinib is metabolized mainly by CYP3A4 in humans, which is the most similar to Cyp3a11 in mice, having 76 % amino acid homology [27]. It has been reported that CYP3A4 displays circadian rhythms and the mechanisms are related to the regulation of the D-site-binding protein (DBP), which is an activate component of the mammalian

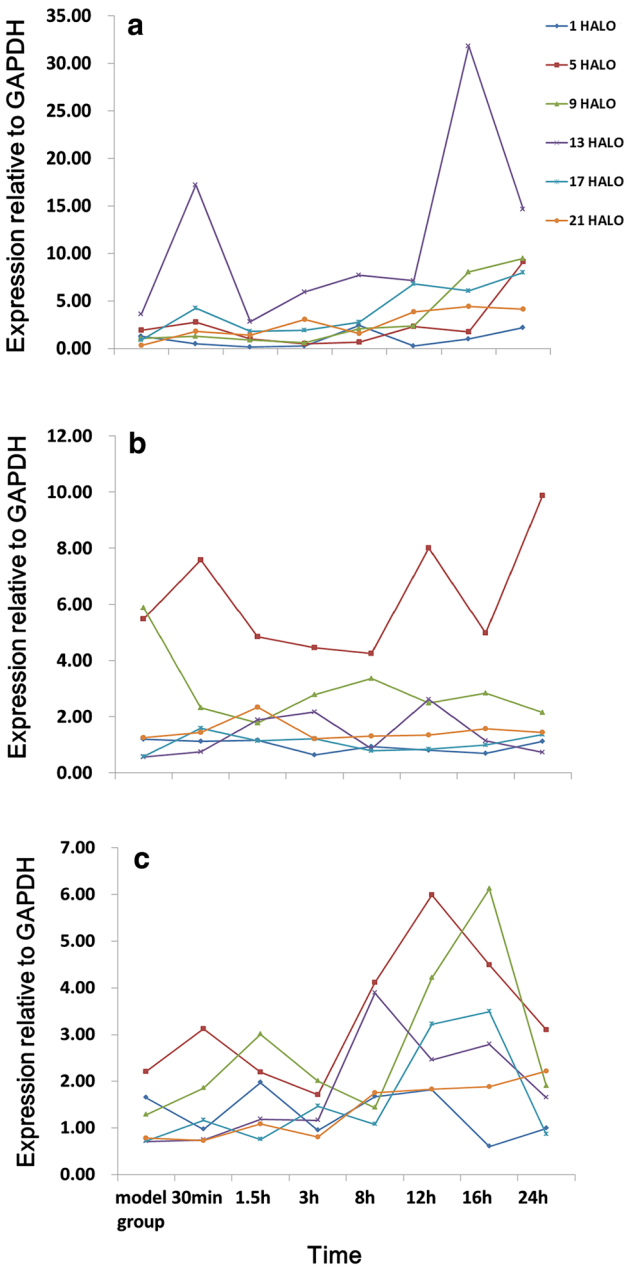

Fig. 3 Comparison of *Cyp1a2*, *Cyp3a13* and *Cyp3a11* mRNA expressions among the six circadian groups. **a** Comparison of *Cyp1a2* mRNA expressions among the six circadian groups. **b** Comparison of *Cyp3a13* mRNA expressions among the six circadian groups. **c** Comparison of *Cyp3a11* mRNA expressions among the six circadian groups

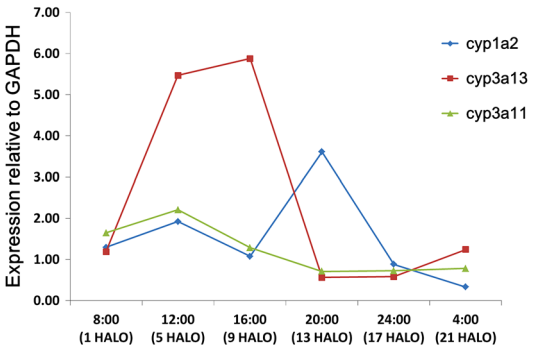

Fig. 4 Variation tendency of *Cyp1a2*, *Cyp3a13* and *Cyp3a11* mRNA expressions of the modeling groups during 24 h

circadian clock [28]. The *Dbp* gene has been identified as a direct target for rhythmic BMAL1 and CLOCK binding [29, 30]. Stratmann et al. [31] have discovered a special BMAL1-binding site in the promoter region of the *Dbp* gene to regulate the phase of its expression according to the photoperiod. Indeed, computer-aided analysis identified a putative DBP-binding site in the promoter region of mouse *Cyp3a11*, which is highly conserved between human and mouse [28, 32]. Based on our observations, even though no significant ups and downs were found in mRNA expression of *Cyp3a11* during 24 h normally, this is still something we should not have ignored. Figure 3 shows that obvious uniformity was exhibited among all six groups in the expression variation of *Cyp3a11* with time (the peak values appeared at about 8–16 h after every administration), which indicated the mRNA expression of Cyp3a11 may be effected by erlotinib. This means that no matter when the drug was given during 1 day, the mRNA expression of *Cyp3a11* will reach a relative peak value at 12–16 h after administration. Previous reports had demonstrated that erlotinib is a moderate inhibitor of CYP3A4, and a potent inhibitor of CYP1A2, which seemed inconsistent with our study. In humans and dogs, rifampicin is a strong inducer of CYP3A4, but not in rats and mice [33]. Thus, the effect of erlotinib on the enzymes may be different between human and mouse. However, our assumption warrants further investigation.

The daily variations in *Cyp3a11*, *Cyp3a13* and *Cyp1a2* expressions may partially explain why the pharmacokinetics of erlotinib varies with its dosing time. In addition, there has been evidence that the blood flow rate to the liver also shows circadian rhythms, which can cause variations in the pharmacokinetics of medications as well [34]. The mRNA expression of the three drug-metabolizing enzymes and the organ blood flow had a significant peak in the active phase (the dark period), leading to a relatively high CL and low T_{max} in the 20:00 and 24:00 groups. Therefore, the drug absorption and elimination were both fast.

Our study showed significant differences in the pharmacokinetics of erlotinib in tumor-bearing mice when it was administered at different times of day. Circadian variations in the absorption, distribution, metabolism and excretion of drugs may be responsible for circadian variations in drug effects and/or side effects [35]. Thus, it is necessary to further investigate the chronopharmacokinetics of erlotinib in clinical practice.

Acknowledgments The authors would like to thank Mr. Jian-Xin Sun and Mr. Lin-Xiang Guo for proofreading this article.

Conflict of interest The authors declare that they have no competing interests. The authors alone are responsible for the content and writing of the paper.

References

1. Hastings MH, Reddy AB, Maywood ES. A clockwork web: circadian timing in brain and periphery, in health and disease. Nat Rev Neurosci. 2003;4(8):649–61.
2. Martin RJ, Banks-Schlegel S. Chronobiology of asthma. Am J Respir Crit Care Med. 1998;158(3):1002–7.
3. Smolensky MH, Lemmer B, Reinberg AE. Chronobiology and chronotherapy of allergic rhinitis and bronchial asthma. Adv Drug Deliv Rev. 2007;59(9–10):852–82.
4. Smolensky MH, Reinberg A, Labrecque G. Twenty-four hour pattern in symptom intensity of viral and allergic rhinitis: treatment implications. J Allergy Clin Immuno. 1995;95(5 Pt 2):1084–96.
5. Portaluppi F, Hermida RC. Circadian rhythms in cardiac arrhythmias and opportunities for their chronotherapy. Adv Drug Deliv Rev. 2007;59(9–10):940–51.
6. Portaluppi F, Lemmer B. Chronobiology and chronotherapy of ischemic heart disease. Adv Drug Deliv Rev. 2007;59(9–10):952–65.
7. Levi F, Focan C, Karaboue A, de la Valette V, Focan-Henrard D, Baron B, Kreutz F, Giacchetti S. Implications of circadian clocks for the rhythmic delivery of cancer therapeutics. Philos Trans A Math Phys Eng Sci. 2008;366(1880):3575–98.
8. Savvidis C, Koutsilieris M. Circadian rhythm disruption in cancer biology. Mol Med. 2012;18:1249–60.
9. Ayala DE, Hermida RC. Sex differences in the administration time-dependent effects of low-dose aspirin on ambulatory blood pressure in hypertensive subjects. Chronobiol Int. 2010;27(2):345–62.
10. Hermida RC, Ayala DE, Mojon A, Fernandez JR. Ambulatory blood pressure control with bedtime aspirin administration in subjects with prehypertension. Am J Hypertens. 2009;22(8):896–903.
11. Hermida RC, Ayala DE, Mojón A, Chayán L, Domínguez MJ, Fontao MJ, et al. Comparison of the effects on ambulatory blood pressure of awakening versus bedtime administration of torasemide in essential hypertension. Chronobiol Int. 2008;25(6):950–70.
12. Hermida RC, Ayala DE. Chronotherapy with the angiotensin-converting enzyme inhibitor ramipril in essential hypertension:improved blood pressure control with bedtime dosing. Hypertension. 2009;54(1):40–6.
13. Hermida RC, Ayala DE, Fontao MJ, Mojon A, Fernandez JR. Chronotherapy with valsartan/amlodipine fixed combination: improved blood pressure control of essential hypertension with bedtime dosing. Chronobiol Int. 2010;27(6):1287–303.
14. Buttgereit F, Doering G, Schaeffler A, Witte S, Sierakowski S, Gromnica-Ihle E, et al. Targeting pathophysiological rhythms: prednisone chronotherapy shows sustained efficacy in rheumatoid arthritis. Ann Rheum Dis. 2010;69(7):1275–80.
15. Tharavanij T, Wongtanakarn S, Lerdvuthisopon N, Teeraaunkul S, Youngsriphithak P, Sritipsukho P. Lipid lowering efficacy between morning and evening simvastatin treatment: a randomized double-blind study. J Med Assoc Thail. 2010;937 (suppl):S109–13.
16. Almeida L, Loureiro AI, Vaz-da-Silva M, Torrão L, Maia J, Fernandes-Lopes C. Chronopharmacology of nebicapone, a new catechol-*O*-methyltransferase inhibitor. Curr Med Res Opin. 2010;26(5):1097–108.
17. Okeahialam B, Ohihoin E, Ajuluchukwu J. Chronotherapy in Nigerian hypertensives. Ther Adv Cardiovasc Dis. 2011;5(2):113–8.
18. Harris B, Song R, Soong SJ, et al. Relationship between dihydropyrimidine dehydrogenase activity and plasma 5-fluorouracil levels with evidence for circadian variation of enzyme activity and plasma drug levels in cancer patients receiving 5-fluorouracil by protracted continuous infusion. Cancer Res. 1990;50(1):197–201.
19. Zhou C, Wu YL, Chen G, Feng J, Liu XQ, Wang C, et al. Erlotinib versus chemotherapy as first-line treatment for patients with advanced EGFR mutation-positive non-small-cell lung cancer (OPTIMAL, CTONG-0802): a multicentre, open-label, randomised, phase 3 study. Lancet Oncol. 2011;12(8):735–42.
20. Filipski E, Lemaigre G, Liu XH, Méry-Mignard D, Mahjoubi M, Lévi F. Circadian rhythm of irinotecan tolerability in mice. Chronobiol Int. 2004;21(4–5):613–30.
21. Portaluppi F, Smolensky MH, Touitou Y. Ethics and methods for biological rhythm research on animals and human beings. Chronobiol Int. 2010;27(9–10):1911–29.
22. Tampellini M, Filipski E, Liu XH, Lemaigre G, Li XM, Vrignaud P, et al. Docetaxel chronopharmacology in mice. Cancer Res. 1998;58:3896–904.
23. Zhao J, Lu J, Yang H-Y, Zhao J-M, Zhai J-M, Li S, et al. A comparative study on the ways of building the Lewis lung carcinoma animal models. Cancer Res Clin. 2008;20(7):439–41.
24. Faivre L, Gomo C, Mir O, Taieb F, Schoemann-Thomas A, Ropert S, et al. A simple HPLC-UV method for the simultaneous quantification of gefitinib and erlotinib in human plasma. J Chromatogr B. 2011;879(23):2345–50.
25. Schmutz I, Albrecht U, Ripperger JA. The role of clock genes and rhythmicity in the liver. Mol Cell Endocrinol. 2012;349(1):38–44.
26. Zhang YK, Yeager RL, Klaassen CD. Circadian expression profiles of drug-processing genes and transcription factors in mouse liver. Drug Metab Dispos. 2009;37(1):106–15.
27. Yanagimoto T, Itoh S, Muller-Enoch D, Kamataki T. Mouse liver cytochrome P-450 (P-450IIIAM1): its cDNA cloning and inducibility by dexamethasone. Biochim Biophys Acta. 1992;1130(3):329–32.
28. Takiguchi T, Tomita M, Matsunaga N, Nakagawa H, Koyanagi S, Ohdo S. Molecular basis for rhythmic expression of CYP3A4 in serum-shocked HepG2 cells. Pharmacogenet Genomics. 2007;17(12):1047–56.
29. Kiyohara YB, Nishii K, Ukai-Tadenuma M, Ueda HR, Uchiyama Y, Yagita K. Detection of a circadian enhancer in the mDbp promoter using prokaryotic transposon vector-based strategy. Nucleic Acids Res. 2008;36(4):e23.
30. Ripperger JA, Schibler U. Rhythmic CLOCK-BMAL1 binding to multiple Ebox motifs drives circadian Dbp transcription and chromatin transitions. Nat Genet. 2006;38(3):369–74.
31. Stratmann M, Stadler F, Tamanini F, van der Horst GT, Ripperger JA. Flexible phase adjustment of circadian albumin D site-binding protein (DBP) gene expression by CRYPTOCHROME1. Genes Dev. 2010;24(12):1317–28.
32. Min DI, Chen HY, Lee MK, Ashton K, Martin MF. Time-dependent disposition of tacrolimus and its effect on endothelin-1 in liver allograft recipients. Pharmacotherapy. 1997;17(3):457–63.
33. Vignati LA, Bogni A, Grossi P, Monshouwer M. A human and mouse pregnane X receptor reporter gene assay in combination with cytotoxicity measurements as a tool to evaluate species-specific CYP3A induction. Toxicology. 2004;199(1):23–33.

34. Ben-Cherifa W, Dridi I, Aouam K, Ben-Attia M, Reinberg A, Boughattas NA. Circadian variation of valproic acid pharmacokinetics in mice. Eur J Pharm Sci. 2013;49(4):468–73.

35. Baraldo M. The influence of circadian rhythms on the kinetics of drugs in humans. Expert Opin Drug Metab Toxicol. 2008;4(2):175–92.